Nat Hazards
DOI 10.1007/s11069-014-1088-5

ORIGINAL PAPER

A new monitoring station for debris flows in the European Alps: first observations in the Gadria basin

F. Comiti · L. Marchi · P. Macconi · M. Arattano · G. Bertoldi · M. Borga · F. Brardinoni · M. Cavalli · V. D'Agostino · D. Penna · J. Theule

Received: 19 March 2013 / Accepted: 8 February 2014
© Springer Science+Business Media Dordrecht 2014

Abstract Debris-flow monitoring in instrumented areas is an invaluable way to gather field data that may improve the understanding of these hazardous phenomena. A new experimental site has been equipped in the Autonomous Province of Bozen-Bolzano (Eastern Alps, Italy) for both monitoring purposes and testing early warning systems. The study site (Gadria basin) is a 6.3 km^2 catchment subjected to frequent debris flows. The monitoring system in the Gadria basin consists of rain gauges, radar sensors, geophones, video cameras, piezometers and soil moisture probes. Transmission of data and alerts from the instruments exploits in part radio technology. The paper presents the data gathered

Electronic supplementary material The online version of this article (doi:10.1007/s11069-014-1088-5) contains supplementary material, which is available to authorized users.

F. Comiti (✉) · D. Penna · J. Theule
Faculty of Science and Technology, Free University of Bozen-Bolzano, Piazza Università 5, 39100 Bolzano, Italy
e-mail: Francesco.comiti@unibz.it

L. Marchi · M. Cavalli
Research Institute for Geo-hydrological Protection, National Research Council of Italy, Corso Stati Uniti 4, 35127 Padova, Italy

P. Macconi
Department of Hydraulic Engineering, Autonomous Province of Bozen-Bolzano, via Cesare Battisti 23, 39100 Bolzano, Italy

M. Arattano
Research Institute for Geo-hydrological Protection, National Research Council of Italy, Strada delle Cacce 73, 10135 Torino, Italy

G. Bertoldi · M. Borga · V. D'Agostino · D. Penna
Department of Land, Environment, Agriculture and Forestry, University of Padova, viale dell'Università 16, 35020 Legnaro, PD, Italy

F. Brardinoni
Department of Earth and Environmental Sciences, University of Milano Bicocca, Piazza della Scienza 1, 20126 Milano, Italy

during the first three years of activity, with two debris-flow events recorded at the station varying in magnitude and characteristics, and discusses the perspectives of debris-flow monitoring and related research.

Keywords Debris flow · Instrumental monitoring · Flow velocity · Soil moisture · Alps

1 Introduction

Debris flows represent one of the most relevant natural hazards in mountainous regions. In Europe, debris flows cause extensive damages and casualties every year (Guzzetti et al. 2005; Hilker et al. 2009). Construction of residential buildings and transport infrastructures on debris-flow fans has progressively increased the vulnerability to such events, thus augmenting the overall risk. The quantification of sediment volumes transported by debris flows, along with their temporal frequency, timing, flow characteristics (i.e., velocity, flow depth, density), is of crucial importance for hazard assessment, land-use planning and design of torrent control structures. For this aim, long-term instrumental observations of debris flows are of extreme value, similarly to experimental stations for bedload transport (see e.g., Mao et al. 2009; Rickenmann et al. 2012). In addition, instrumented basins provide high-quality information for deriving regional thresholds of rainfall intensity and/or cumulative values for debris-flow triggering to be used in warning systems.

Japan and China have pioneered debris-flow monitoring (Okuda et al. 1980; Zhang 1993) with instrumented sites that still play a significant role in debris-flow research, thanks to the long time series of recorded data (Hu et al. 2011; Suwa et al. 2011). The frequent occurrence of high-magnitude debris flows with severe damages to settlements in Taiwan has urged the installation of equipment for monitoring debris flows and for issuing warnings in a number of sites (Yin et al. 2011). Among early experiences on instrumental observations of debris flows in the United States are the monitoring campaigns by Pierson (1986) in channels on the flanks of Mount St. Helens. More recently, the installation of monitoring equipment at Chalk Cliffs, a small, very active catchment in the Colorado Rocky Mountains, has started providing valuable information on debris-flow triggering and flow dynamics (Coe et al. 2008; McCoy et al. 2010). In Europe, the first catchment instrumented for debris-flow monitoring was probably the Moscardo Torrent in the Eastern Italian Alps (Marchi et al. 2002). Other sites were instrumented in the late 1990s and early 2000s in Italy (Tecca et al. 2003) and Switzerland (Hürlimann et al. 2003). Among these sites, the Illgraben catchment (Switzerland) deserves to be mentioned, especially because of innovative measurements on forces and pore fluid pressure in debris flows (McArdell et al. 2007) and channel-bed erosion (Berger et al. 2011). Recent development of monitoring activities in Europe, which include installations in Austria (Kogelnig et al. 2014), France (Navratil et al. 2012, 2013) and Spain (Hürlimann et al. 2011), indicates the high interest for this sector of debris-flow studies. The number of monitoring sites and the amount of recorded data on debris flows, however, still remain limited if compared to landslides and fluvial sediment transport. Moreover, the large variability of debris-flow features, their dependence on local topographic, geologic and climatic conditions makes the collection of more data in instrumented catchments of the utmost importance.

Structural measures such as check dams, retention basins, dikes and artificial channels have been built for decades in order to stop, divert or “flush” debris flow from sensitive locations. Although these hydraulic works still represent the core of debris-flow control interventions for protecting urban areas and main transportation routes, they present several management problems and cannot be systematically implemented. Economic constraints also exist when the elements at risk are spread over a large area. It is now recognized that a combination of structural and non-structural measures is needed in most cases to cope with debris-flow risks. Non-structural measures mainly aim to diminish the vulnerability of a certain area from the debris-flow processes, by reducing either permanently (e.g., land-use planning) or temporarily (warning systems) the probability that humans and their goods might be hit by a debris flow.

Warning systems for debris flows can be classified into two main types: advance warning and event warning (Hungr et al. 1987; Arattano and Marchi 2008). Advance warning systems predict the possible occurrence of a debris flow beforehand, by monitoring the possible onset of triggering conditions. These warnings are usually obtained by comparing precipitation forecasts with locally available precipitation thresholds for triggering (e.g., Caine 1980; Wilson et al. 1993; Bacchini and Zannoni 2003; Guzzetti et al. 2008, Staley et al. 2013). On the one hand, these approaches permit lead times of some hours. On the other hand, the warnings are heavily affected by the uncertainties in the precipitation forecasts and in the estimates of local threshold curves. An event warning is issued after the actual detection of debris flows, based on measures from wire sensors, ground vibration sensors or stage meters (Arattano and Marchi 2008), upstream of a precisely defined vulnerable site (e.g., road, town). Owing to such characteristics, event warning is potentially highly reliable (Chang 2003; Badoux et al. 2009), even though the time interval between the detection and the arrival of the debris flow to the vulnerable site is very short and, in addition, the need of maintenance increases the costs. These limitations are intrinsic to debris-flow warning systems and cannot be easily eliminated, but refinements in debris-flow detection and alarm dissemination technologies may contribute to improve the warning effectiveness.

In this paper, we present a new experimental station which has been recently installed in the Eastern Italian Alps in order to both monitor debris flow and to test warning systems. Data obtained through this permanent monitoring facility will provide further knowledge on debris-flow behavior, will enhance the investigations on their rheological behavior and will permit to calibrate numerical models for simulating their propagation (Arattano and Franzi 2004; Arattano et al. 2006). Also, warning algorithms to detect in advance the arrival of debris flows are being tested, in particular with the use of geophones that have already proved to be able to detect the arrival of the debris-flow front earlier than its actual transit at the sensor site (Arattano 2003).

The main aim of the present paper is twofold: (i) to describe the technical solutions adopted for the monitoring station; and (ii) to present the first experimental data gathered during the period 2011–2013.

2 The study basin

The station for monitoring debris flows and testing warning procedures was installed during spring 2011 at the confluence of the Gadria–Strimm channels, located in the Vinschgau-Venosta valley, Autonomous Province of Bozen-Bolzano, Italy (Fig. 1). Even though the monitored debris flows are originated from the Gadria basin alone, some instrumentation is also installed in the Strimm catchment to enhance the hydrological information on debris flow in the neighboring catchment. Therefore, both Gadria and Strimm basins are described in this section.

The Gadria catchment has a drainage area of 6.3 km^2, ranges in elevation from 1,394 to 2,945 m a.s.l., features an average slope of 79.1 % and is the focus of most monitoring

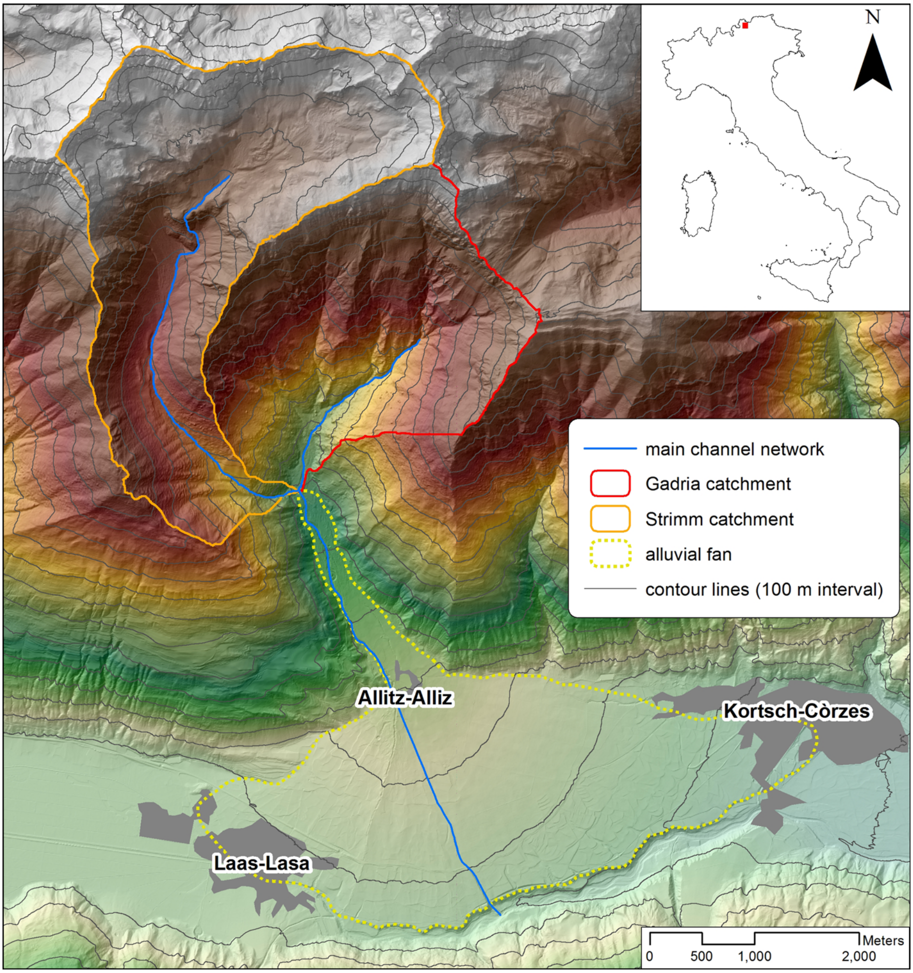

Fig. 1 Map and location of the Gadria–Strimm catchments

activities. The Strimm basin (area 8.5 km^2, maximum elevation 3,197 m a.s.l., average slope 61.8 %) joins the Gadria at a filter check dam located near the apex of their large alluvial fan (10.9 km^2). The combination of steep topography, highly deformed/fractured metamorphic rocks and thick glacio-fluvial deposits, sets the conditions for chronic debris-flow activity within the Gadria channel network.

2.1 Climate

The site is characterized by the driest inner-Alpine climate (Frei and Schär 1998), with mean annual precipitation (MAP) as low as 480 mm in the Vinschgau valley floor (data from the station of Laas-Lasa, 863 m a.s.l., period 1989–2012), due to the sheltering effect of the mountainous ranges to southerly and northerly winds. MAP increases strongly with altitude over the Gadria–Strimm basins, with 662 mm measured at a rain gauge located at 1,754 m a.s.l. (period 1993–2012). Long-term series are not available for the elevation band of 2,000–2,500 m a.s.l., where a large part of sediment sources is located. An estimate of about 800–900 mm MAP is obtained for these elevations based on short records. A strong altitude dependency is observed also for the subdaily rainfall extremes (Parajka et al. 2010). At Laas, a maximum of 46 mm in 24 h, 24 mm in 1 h and 21 mm in 15 min was recorded in the period 1989–2012. At the 1,754 m a.s.l station, the maximum daily precipitation recorded in the period 1993–2012 amounts to 72 mm (hourly or subhourly precipitation data are not available). Snow cover usually lasts from mid-November to mid-April, and summer convective storms are responsible for most of the debris-flow events.

2.2 Geology

The central part of the Vinschgau valley, a glacial trough that sits within the Austroalpine nappe stack between the Engadine and the Periadriatic lineaments (Ratschbacher 1986; Thöni 1999; Solva et al. 2005), has a geology dominated by metamorphic lithologies. In this context, the Ötztal unit and the underlying Campo nappe chiefly consist of gneiss and schist, with subordinate amphibolites, orthogneiss and marble, separated by Permo-Mesozoic metasedimentary rocks. Mylonitic and cataclastic layers are common along the principal tectonic lineaments (Thöni 1999; Bargossi et al. 2010). The Ötztal-Campo stack is characterized by fractures trending along N, E, NE and SW directions, and these structural patterns impart a primary control on the spatial structure of the drainage network and influence rock strength.

Most of Strimm basin and the upper portion of Gadria basin are underlain by paragneiss of the Mazia unit. This lithology presents frequent pegmatitic intrusions with adjacent phyllonitic transitions, result of Permiam low-grade metamorphism (Habler et al. 2009). The southern part of the study area is dominated by orthogneiss showing mylonitic character as one approaches the Vinschgau-Venosta Shear Zone. The presence of thick Quaternary deposits makes the spatial delineation of the transition between the two units particularly difficult.

2.3 Geomorphology

Periglacial activity is prevalent in the hanging valley that forms the upper half of Strimm basin as witnessed by a number of active rock glaciers. Fluvial transport dominates along the main stem of Strimm Creek, and colluvial processes operate through a number of mechanisms including shallow debris slides and debris avalanches, which at times can transform into in-channel debris flows, as well as rockfalls, rock slides and dry ravel on the steep rocky slopes feeding talus slopes and debris cones. Of particular interest are the massive kame terraces located along the steep headwalls of Gadria Creek. They sit on extremely weathered and fractured bedrock surfaces, which have developed steep ravines and badland-like morphology since the glacial retreat. Such an unstable setup provides a virtually unlimited source of sediment to the high debris-flow activity observed along Gadria Creek. Figure 2 shows some views of the Gadria basin.

The spatial characterization of connectivity patterns in the entire Strimm–Gadria catchment has been analyzed through a topographic-based index by Cavalli et al. (2013). The Strimm and Gadria catchments are remarkably distinct in the efficiency of sediment routing. The Strimm basin presents a wide low-slope area—a hanging valley—that is poorly connected to the basin outlet, whereas the lower part of the basin displays a higher degree of connectivity to the outlet. In contrast, the Gadria basin is characterized by a more homogeneous pattern with generally a higher degree of sediment connectivity starting from

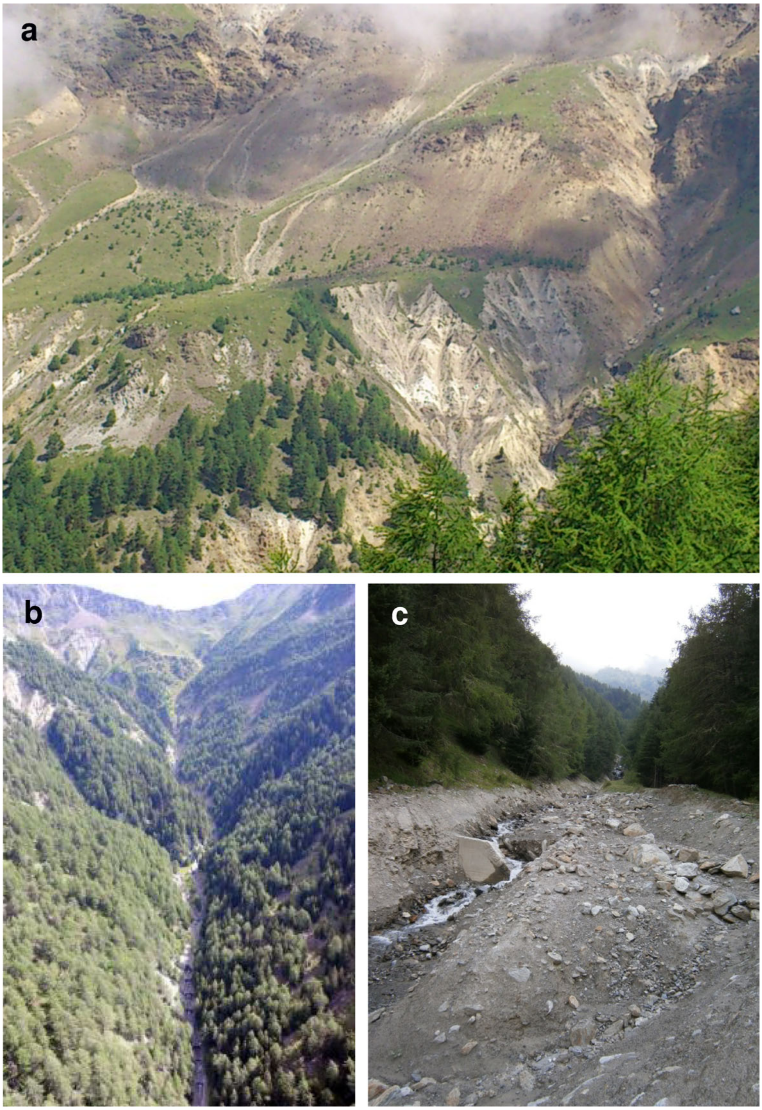

Fig. 2 Views of the Gadria basin: **a** kame terraces deposited over highly weathered bedrock, close to site S1 in Fig. 3 (note development of badland-like features on bedrock outcrops); **b** the main channel upstream of the surveyed reach displayed in Fig. 3, featuring many consolidation check dams; **c** the main channel within the surveyed reach

the upper part of the catchment, suggesting that gullies and deeply incised channels in this sector can play an important role in delivering sediment to the outlet.

The alluvial fan connecting the Gadria–Strimm system to the Etsch-Adige river valley floor belongs to the biggest cluster of anomalously large fans within the European Alps (Fischer 1965), the origin of which is still matter of debate. According to Jarman et al. (2011), on the basis of morphometric analyses and identification of first-order cavities in the relevant source basins, these fans would be the result of giant catastrophic rock failures. On the other hand, paraglacial evacuation of glacial and glacio-fluvial deposits, and downstream fan progradation due to debris-flow activity, might represent a valid alternative, as testified by the strong positive correlation between contemporary debris-flow sediment flux and fan area at the regional scale (Brardinoni et al. 2012), and by the presence of largely eroded kame terraces in the Gadria headwaters.

2.4 Debris-flow mitigation interventions

Regarding human interventions in the basin, in the late nineteenth century, a straight paved channel was built to divert the Strimm–Gadria channel on the fan farther from the village of Laas (see Fig. 1), which had been flooded and hit by debris flows several times. In addition, consolidation check dams were built along the main channels and their headwater tributaries starting in the early twentieth century—nowadays the Gadria main channel and its tributaries feature more than 100 consolidation check dams with different levels of functionality—and finally, in the 1970s, a filter check dam with a storage basin of 40,000–60,000 m^3 (for deposition angles in the range 2°–6°) was built at the fan apex, where now the main monitoring station is located. This work prevents debris flows from propagating onto the fan, but it requires very high maintenance costs for the Province (about 200,000 €/year) due to sediment removal and disposal. In fact, the recent (since 2003), well-documented records of debris flows in the Gadria basin indicate an average of 1–2 events per year, with volumes from 700 to 40,000 m^3 per event (values assessed at the debris retention basin).

3 The monitoring installation

The monitoring systems in the Gadria–Strimm basin consists of rain gauges, radar sensors, geophones, video cameras, piezometers and soil moisture probes. Sensors were installed in spring 2011 both in the Gadria and in the Strimm basin (Fig. 3), but the core of the monitoring lies within the Gadria as this is the channel featuring debris flows. Most of the monitoring equipment was purchased and installed by the department of Hydraulic Engineering of the Autonomous Province of Bozen-Bolzano, with some instruments acquired and maintained by the Free University of Bozen-Bolzano. All the instrumentation installed so far (January 2014) is listed in Table 1. There are both stand-alone instruments and sensors connected to a server, as specified below.

Rainfall is monitored in the Gadria basin by three rain gauges placed at different elevations (locations R1 at 2,160 m a.s.l., R2 at 2,320 m a.s.l., R3 at 1,500 m a.s.l., see Fig. 3), which store precipitation data at 1-min intervals locally and also radio transmits the data to the server (see below). Two additional stand-alone rain gauges are located in the Strimm basin (R4 at 2,080 m a.s.l., R5 at 2,560 m a.s.l.). Unfortunately, the radar coverage of the Gadria basin by means of the weather radar antenna operated by the Autonomous Province of Bozen-Bolzano (Monte Macaion) is severely blocked by intervening orographic obstacles. However, radar-based rainfall estimation could be obtained from a privately managed radar located on the Valluga peak (2,809 m) in Austria.

Debris-flow depth is monitored by stage radar sensors mounted on cable-suspended sledges at three cross-sections (D2, D3, D4) along the Gadria main channel (Fig. 4), and data are recorded in the dataloggers at 1-s time intervals and transmitted to the server.

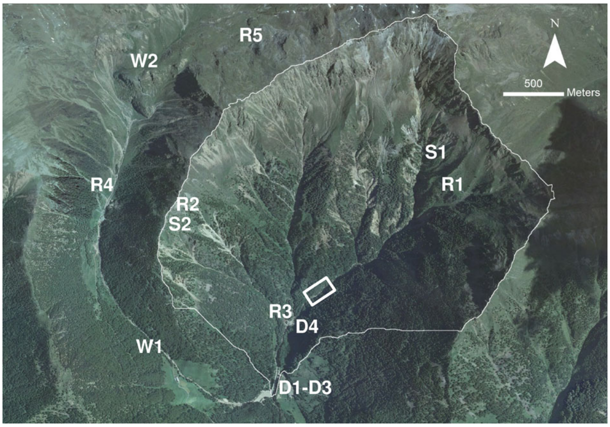

Fig. 3 View of the Gadria (and partly of the Strimm) watershed with the location of the different installation sites (see Table 1). The reach surveyed topographically mentioned in Sect. 4.1 is marked with a *rectangle*

Table 1 Instrumentation installed in the Gadria–Strimm basins

Type of instrument	Brand and model	Location*	Number	Time interval
Rain gauge	Lambrecht 1518	R1, R2, R3, R4	4	1 min
Rain gauge	Campbell Arg100	R5	1	10 min
Radar sensor	Vegapulse 68	D2, D3, D4	3	1 s
Geophone	Pasi 10 HZ SIS-902-050	D2, D3, D4	5	1 s
Video camera	Mobotix M12	D1, D2	3	10 fps
Pressure transducer	Keller DCX-22 VG	W1, W2, S2	8	10 min
Pressure transducer	OTR OG200/R	S1	6	10 min
FDR moisture probe	Spectrum SM100	S2	28	10 min

* As in Fig. 3

However, only the two lower radar sensors were operational in 2011–2013. Radar stage data are used to calculate the mean velocity of debris flows based on the inclined distance between D3 and D2 (80 m measured along the thalweg, a reach representative for debris flows along a sequence of consolidation check dams, with an average bed slope of 16 %).

Vertical geophones (featuring 10 Hz frequency) were installed at the same locations of the radar sensors in the Gadria channel and have been operational since 2012. The choice to use geophones with a natural frequency of 10 Hz was made examining the data available in literature on the frequency ranges of the ground vibrations produced by debris flows. The installed geophones provide a flat response proportional to ground velocity only above the frequency of 10 Hz and a response falling at 12 dB/octave below. LaHusen (1996) found that the typical peak frequencies of a debris-flow wave range between 30 and 80 Hz. Huang et al. (2007) observed, with a greater detail, that at the surge peak, frequencies range between 10 and 30 Hz, while at the flow tail, they range between 60 and 80 Hz. Therefore,

Fig. 4 Aerial view of the lower reaches of the Gadria Creek with stations D1–D3. The server recording all the data and the videos (main station) is located on the left bank close to D2

the 10 Hz geophones should be the most suited for debris-flow monitoring, as they cover the entire expected frequency range.

Locations D2 and D3 feature two geophones each, one placed on loose soil and one attached to the concrete wing of consolidation check dams, in order to investigate their different response to debris flow-induced vibrations. Location D4 has only one geophone installed on the right wing of a large check dam. Geophones are meant to provide a different way—beside radar sensors—to determine debris-flow velocity (Arattano and Marchi 2008) and also magnitude, after their calibration against flow stage and/or possibly against directly deposited volumes. Geophone signal is currently analyzed in terms of mean wave amplitude, recorded every 1 s on the datalogger, following the same approach deployed for the Moscardo Torrent (Arattano and Marchi 2008). However, in this paper, geophone data are not presented due to their availability for one event (July 2013) only.

In order to provide visual information on debris-flow characteristics, three video cameras (resolution 1,024 × 768, at 10 frames per seconds) equipped with spotlights—the latter automatically triggered by the rain gauges located within the basin—were installed at locations D1 (corresponding to the filter check dam mentioned before) and D2 (corresponding to the lowermost radar sensor and geophones). Two video cameras are placed at the former location, one framing the debris retention basin from downstream and one from the left side covering also the confluence of the Strimm Creek, thus enabling the observation of the debris-flow depositions taking place in front of the check dam. The video camera at D2 shoots the channel upstream, i.e., the lower reach monitored by radar sensors and geophones. The debris flows recorded so far occurred during the day, but debris-flow videos at night would be of relatively good quality thanks to the illumination provided by the spotlights.

Finally, to assess the potential relationship between pore water pressure, soil moisture and debris-flow occurrence, two areas in the Gadria catchment were selected to monitor the main hillslope hydrology variables. The first area (Fig. 5a) comprises three steep (inclination 33°–37°) channel heads in the upper part of the watershed (S1 in Fig. 3, elevation about 2,160 m a.s.l.), subject to frequent raveling and characterized by the absence of developed soils and vegetation, non-cohesive loose sediment ranging from coarse sand to very large boulders (Fig. 5b). These sites were equipped with six pore pressure transducers placed at 100–130 cm below the ground surface (recording data at 10 min intervals). The most active of these ravines was equipped since late summer 2013 with a video camera—the same model used at station D1–D2—storing videos on a SD card. The recording is activated by an adjacent rain gauge, and the system is powered by a solar panel. The second area (Fig. 5c) for hillslope hydrology monitoring lies below the divide with the Strimm basin, just above a landslide scar (S2 in Fig. 3), at an elevation of about 2,300 m a.s.l. This site was identified to monitor the spatial and temporal variability of water table levels and volumetric soil moisture at different depths on a steep slope (inclination 35°–38°) where soil—although shallow—is present, in contrast to site S1. Grassy vegetation with sparse trees (*Larix decidua*) characterizes the site. Six piezometric wells were manually dug down to 100–140 cm below the surface, each equipped with a pressure transducer (recording every 10 min), and 28 soil moisture sensors (based on Frequency Domain Reflectometry, recording at 10 min intervals) were inserted horizontally in the soil at 10 and 50 cm depth. No permeability tests were conducted so far at S1 and S2 sites.

The instruments at locations D1, D2 and D3 (video cameras, spotlights, radar sensors and geophones with associated dataloggers) are powered by the standard electrical line which was purposely extended from the nearby farms to the main station, which includes the server (8 Terabyte storage capacity) hosted in a sheltering box, receiving and transmitting antennas mounted on a 8-m high pole, gateways, electrical switchboards and a storage room. Importantly, the main station is accessible by normal vehicles, and a uninterruptible power supply (UPS) apparatus guarantees at least 4 h of functioning to video cameras, instruments and to the server in case of power black-out. As the basin is not covered by GSM networks, radio communication is the only way to receive data transmitted from the remote instruments, as well as to send data and alert message to the Internet, to the headquarters of the Civil Protections and to the local Fire Brigade. Full-resolution videos are transmitted directly by cable to the server where they are stored, but then only lower resolution video frames can be sent out from the server due to band capacity limitation. Radar sensors and geophones at D2 and D3 are connected directly via Ethernet cable to the server, whereas data from those at D4 are radio transmitted to the server.

All the instruments installed at locations different than D1, D2 and D3 are supported by batteries (pressure transducers, soil moisture probes) and solar panels (radar and geophone at D4, all the rain gauges). Instruments within the Strimm basin and those for hillslope hydrology monitoring are intended for post-event analysis, and as such only local storage on dataloggers is carried out (i.e., radio transmission is not provided). On the other hand, all the remote instruments transmitting down to the server are equipped with data loggers, in order to avoid data loss in case of radio transmission malfunctioning. Importantly, the system is open to temporary and/or permanent installations for more sensors.

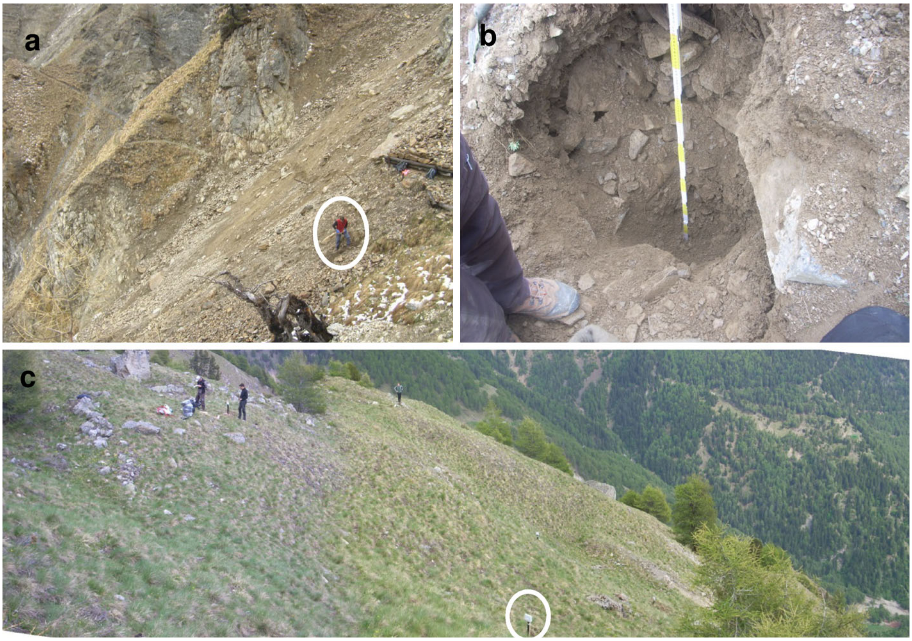

Fig. 5 Images of the sites equipped to monitor hillslope hydrology: **a** the most active channel head at S1 (a person is circled for scale) and **b** the hole where the pore pressure transducer was installed; **c** a panoramic view of site S2 where the soil moisture probes (one datalogger is marked) and piezometers are installed

4 Preliminary results of the monitoring activities (2011–2013)

4.1 General characteristics on the observed debris flows

Two debris flows were recorded at the monitoring station in the period 2011–2013, on August 5, 2011, and on July 18, 2013. In addition, a small debris flow occurred on July 13, 2011, but it did not reach the station as it stopped 900 m upstream of the retention basin. The date of occurrence of this event derives from the field surveys (see below) carried out few days before and after the event, coupled to the precipitation characteristics (intensity and cumulative depth) during the inter-survey period. In 2012, no debris flows were documented in the Gadria basin.

Sediment budgeting and geomorphic monitoring of each event were carried out following the methodology described in Hungr et al. (2005) and Theule et al. (2012). Since 2011, ten cross-sections were repeatedly surveyed—by a range finder mounted on a tripod—on a reach in the middle-lower Gadria channel (Figs. 3, 5c) featuring an average slope of 17 %. The net sediment balance (in m^3 per meter of channel length) was estimated for each of the three events (Fig. 6).

The small July 2011 debris flow caused widespread aggradation along the surveyed reach, with an average positive morphologic change of 4.1 m^3 m^{-1}. The relatively larger event (see next section on magnitudes) occurred in August 2011 displayed an alternation of aggradation and degradation along the reach, with morphologic changes ranging from -12.2 to 15.1 m^3 m^{-1} (average value of 1.2 m^3 m^{-1}). Finally, the largest event observed in July 2013 was mainly erosive in the analyzed reach, with large entrainment in the

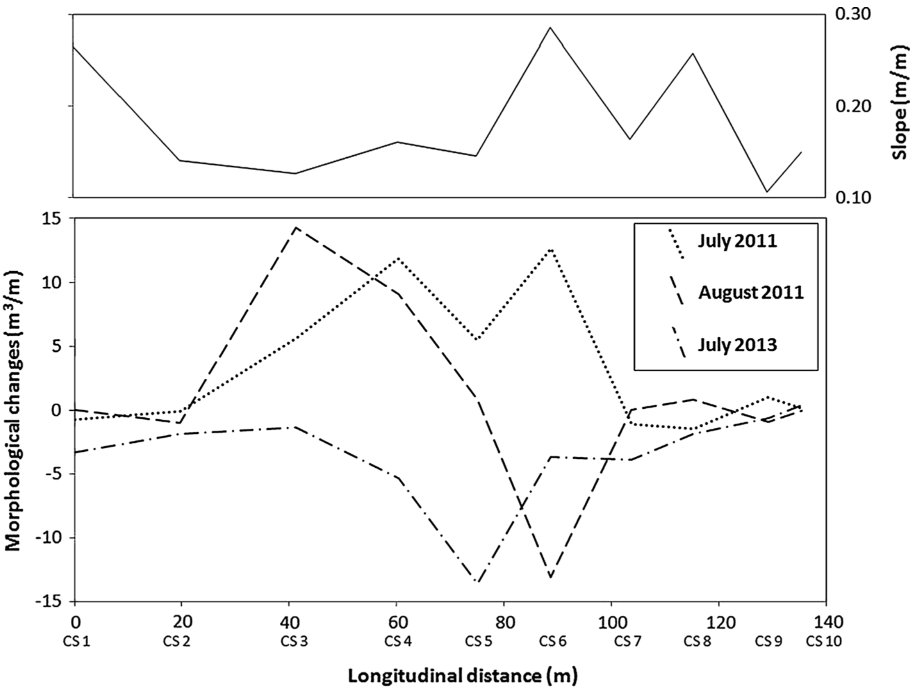

Fig. 6 Erosion/deposition rates (expressed as m^3 per m of channel length) associated with the debris flows detected in a reach upstream of station D4 in the period 2011–2013 (see Fig. 3). Positive values mean deposition, negative erosion. The July 2011 event did not reach the monitoring stations. The upper plot shows the local slope variations within this reach

channel (morphologic change ranges from 0.3 to $-13.6\ m^3\ m^{-1}$, on average $-3.6\ m^3\ m^{-1}$). The relation between aggradation/degradation and local bed slope is partially apparent only for the moderate debris flow of August 2011 (Fig. 6). The average channel slope in the monitored reach (17 %) possibly lies close to the threshold between transport and depositional tendencies, which is affected by event magnitude as well as by antecedent bed conditions.

The three video cameras worked satisfactorily and the radar sensors placed at the sections D2 and D3 (at D4 it was installed later, as mentioned above) provided reliable measurements of the flow depth for both August 2011 and July 2013 events. As also said before, the geophones were not operational yet in 2011 and their data collected in 2013 are not presented here.

The functioning of all but one rain gauge (R1) in the Gadria was hampered in 2011 by technical problems regarding the detachment of the funnel conveying rainfall water to the tipping bucket, and unfortunately, this was discovered only after the event. The rain gauges were replaced in spring 2012. Therefore, rainfall data within the Gadria basin for the July and August 2011 events are available for the rain gauge R1 only. For the former, which did not reach the monitoring station as described above and thus its arrival time is not known, the cumulative rainfall depth of the most intense storm recorded on that day amounts to 5 mm (from 3.10 p.m. to 4.40 p.m.) and max intensity of 2.2 mm in 10 min. Rainfall data available from the rain gauge located in the upper Strimm basin (R5 in Fig. 3) are not considered relevant for this event as this was generated in the portion of the Gadria catchment much closer to the rain gauge R1.

A small rainfall amount was recorded also during the more relevant August 2011 event (9.4 mm, from 2.25 p.m. to 7.40 p.m. when the debris flow arrived at the station, local time), with a maximum intensity of 0.9 mm in 10 min. The weather station run by the Province of Bozen-Bolzano in Laas (located about 4 km south of the Gadria basin, see Fig. 1) recorded 6.4 mm between 6.50 p.m. of August 5 and 3.00 a.m. of August 6 (max intensity 0.4 mm in 10 min). More relevant is the daily rain gauge run by the Province at 1,754 m a.s.l., located near the junction between the Strimm and Gadria channels, which registered a total of 15.4 mm for August 5–6 (i.e., from 9 a.m. to 9 a.m.). The very small precipitation depth, the moderate intensity and the almost negligible rainfall in the 2 h before the debris flow (2.4 mm) might indicate that the rain gauge R1 was outside the area featuring the most intense precipitation during that event. Nonetheless, soil moisture in mid-summer 2011 was relatively high as will be illustrated in Sect. 4.3.

The debris flow of July 2013 was also triggered by a quite limited cumulative rainfall, as the event rainfall depth amounts to 23 mm (in 33 min, at R1), but considering the time when the debris-flow front passed at the monitoring station this reduces to 17.2 mm in only 15 min, with a mean intensity of 69 mm h^{-1} (max of 14.7 mm in 10 min) which is well above the intensity–duration threshold curves determined in other monitoring sites of the Alps (Fig. 7). In contrast, July and August 2011 events plot very close to the lowest threshold curve (McArdell and Badoux 2007). However, because the exact time of occurrence of the July 2011 event is not known, its mean rainfall intensity and duration refer to the entire storm measured on that day and not to the values measured at the arrival of the debris-flow front as in the case of the other events.

Remarkably, the total precipitation measured at the other Gadria rain gauges during the July 2013 event was slightly above 5 mm for a very similar duration, thus plotting well below the threshold (see R3 in Fig. 7). Such a strong spatial gradient in the precipitation field within the Gadria–Strimm basins is confirmed by the weather radar rainfall estimates based on data from the antenna located on the Valluga peak in Austria (Fig. 8). The rainfall map matches the observations that this debris flow originated only in the northeastern portion of the Gadria basin. The grid cell over the rain gauge R1 (see Fig. 3) results with about 32 mm of cumulative rainfall, whereas the value measured at R1 is 23 mm. Both measurements, related to a short-duration cloudburst, indicate high-intensity rainfall. The difference between the two estimates is consistent with their spatial resolution (point measurement by the rain gauge vs. 1 km^2 cell of the weather radar). Unfortunately, Valluga radar data for the 2011 events could not be obtained. In the case of small convective cells triggering debris flows, as in the Gadria, the high spatial variability in rainfall strongly questions the use of warning systems based on intensity–duration thresholds measured at only few rain gauges, unless they are located on all the possible initiation areas for debris flows in a basin.

The hydrographs in the Gadria Creek obtained from the two radar sensors during the August 2011 and July 2013 events (Fig. 9) feature sharp rising limb, quick recession and short durations, as is typical of debris flows, indeed resembling events recorded in other catchments instrumented for debris-flow studies (e.g., Pierson 1986; Zhang 1993; Marchi et al. 2002; Hürlimann et al. 2003; Tecca et al. 2003; McCoy et al. 2010). The August 2011 debris flow consisted of three, relatively small surges (Figs. 9, 10), the first one being slightly more severe; the overall duration of the event was around 25 min. In contrast, the July 2013 event was characterized by a deep (about 2 m), bouldery front followed by a sequence of much smaller and more liquid surges. However, isolated boulders were

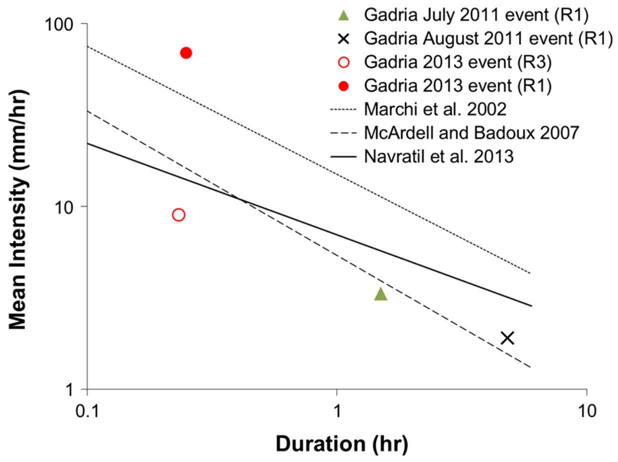

Fig. 7 Rainfall intensity–duration plot showing the July 2011, August 2011 and July 2013 debris flows in the Gadria. Data from the rain gauge at R3 for the 2013 event are remarkably lower than from site R1, whereas only the rain gauge R1 was available for the 2011 events. The point relative to the July 2011 debris flow is based on rainfall depth and duration calculated for the whole storm (and not until the arrival of the initial front) because the exact time of occurrence of this event is not known as it did not reach the station. Threshold curves from different areas of the European Alps are also plotted

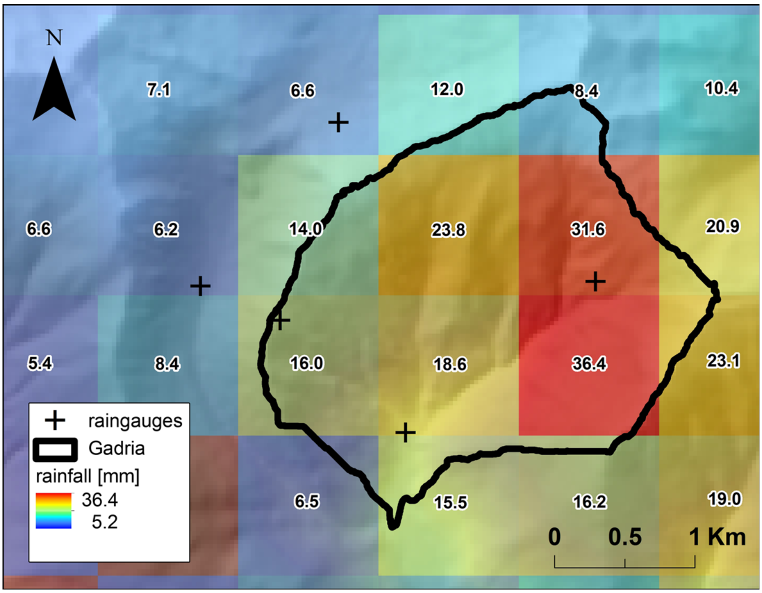

Fig. 8 Cumulative rainfall depth for the July 18, 2013, event derived from the analysis of Valluga weather radar data. The large spatial variability in precipitation over the Gadria basin during this convective storm is evident

observed also during these surges (Fig. 10), as also visible from the radar records (Fig. 9). Remarkably, the flow before the arrival of the initial front in 2013 was steadily low and very clear, as seen in the lower left corner of the upper frame reported in Fig. 10.

4.2 Velocity, peak discharge and volumes of August 2011 and July 2013 events

Debris-flow velocity for the August 2011 and July 2013 events was calculated using two different approaches. The first computed the mean propagation velocity of the front as the ratio of the distance between the instrumented cross-sections (80 m) to the time interval between the arrival of the debris-flow surge at the two gaging stations. The surge arrival was detected using the hydrographs recorded by the two radar sensors. For August 2011, surges 2 and 3 show a unique, well-defined peak, and their mean propagation velocity was computed considering the occurrence of the maximum flow depth in the hydrographs. On the contrary, the first surge displays a rather complex pattern where the flow peak cannot be univocally identified. Therefore, the time interval that has been used as the denominator in the velocity calculation was elapsed between the occurrence of the initial sharp rise of the hydrograph at the two gaging stations. As to the 2013 event, the velocity of the debris-flow front and of subsequent surges was calculated based on the occurrence of the maximum flow depth excluding "spikes" in the hydrographs which are most likely associated with the passage of boulders under the sensors.

The second approach computed the average propagation velocity of each debris-flow surge by cross-correlation (Arattano and Marchi 2005). Cross-correlation can be generally defined as the correlation of a data series with a related one featuring a time lag, permitting to determine the value of this latter through an objective methodology. The time lag between rainfalls and landslide displacements, for instance, can be evaluated through cross-correlation (Lollino et al. 2002, 2006). Because stage records of a debris flow at two different sections can be viewed as two data series shifted by a time lag (i.e., the celerity of propagation), this latter can be estimated through this type of analysis. Arattano et al. (2012) have recently applied cross-correlation for this latter purpose and verified the validity of its results through the analysis of debris-flow hydrographs collected in an instrumented basin. For the August 2011 event, the two approaches give identical velocity values for the first and the third surges (Table 2), whereas cross-correlation provides a slightly lower velocity (1.3 vs. 1.7 m s^{-1}) for the second surge. The difference is within the variations expected by the application of different velocity assessment methods.

A closer assessment of the characteristics of these two events was possible thanks to video recordings, which proved to have fundamental importance to interpret data measured by radar sensors and recognize the features of the various surges (Fig. 10). In the August 2011 event, the first surge was very fluid and turbulent, and these features lead to classify it as a debris flood (Hungr et al. 2001). The second and third surges display instead the distinctive characteristics of debris flows (high density, absence of turbulence, high boulder concentration at the front). Remarkably, the first more fluid surge shows a higher propagation velocity compared to the following, denser ones. In contrast, the July 2013 event presented an initial boulder-rich front moving at a high velocity (5.7 m s^{-1}), whereas the following surges, even if more liquid, feature lower velocities (ranging approximately from 1 to 4 m s^{-1}) probably as a result of much smaller depths. For this event, cross-correlation analysis provides a mean propagation velocity of the whole debris flow of 5.0 m s^{-1}.

Peak discharge of the two debris flows was computed as the product of surge velocity by the flow's cross-sectional area, surveyed by a total station after the event at station D2. The presence of the check dam at D2 makes the cross-section stable, inhibiting significant vertical and lateral erosion. The videos also permitted to exclude the occurrence of significant deposits that might have affected the discharge estimation.

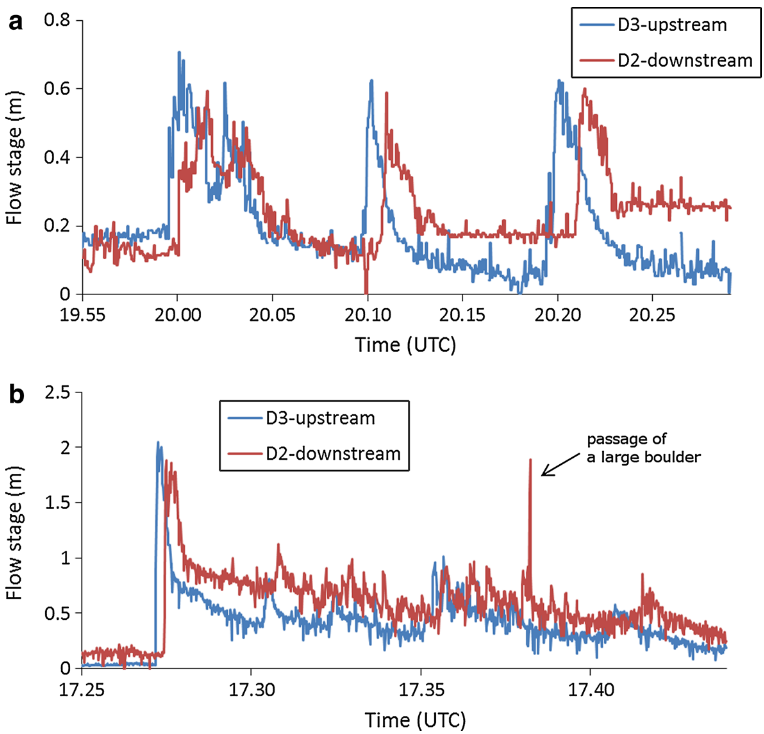

Fig. 9 Radar hydrographs (stations D2 and D3) of the August 5, 2011 (**a**) and July 18, 2013 (**b**) debris flows

The bulked volumes of each surge were calculated as:

$$\text{Vol} = v \cdot \sum_{t_0}^{t_e} A(t) \tag{1}$$

where Vol is the discharged volume during a surge (m^3); $A(t)$ is the cross-sectional area at the time t; v is flow velocity of the surge; t_0 and t_e represent the initial and final time of the surge, respectively. Assumptions and approximations of this approach to debris-flow peak discharge and volume estimation (e.g., variations in flow velocity during the surge transit) are discussed in Marchi et al. (2002).

Table 2 Peak discharge and volume for the debris flow of August 5, 2011

Surge no.	Initial time	Final time	Mean flow velocity of the peak (m s^{-1})	Mean flow velocity of the surge* (m s^{-1})	Peak discharge (m^3 s^{-1})	Volume (m^3)
1	19.59.43	20.06.15	2.6	2.6	11.3	1,749
2	20.10.11	20.12.42	1.7	1.3	4.8	249
3	20.20.01	20.24.21	1.0	1.0	3.8	418

* From cross-correlation

Fig. 10 Frames from the video camera at station D2. *Left column*: the three surges of August 2011 event (surge 1 above, surge 2 in the middle and surge 3 below, as in Table 2); *right column*: three snapshots of the July 2013 debris flow, with the initial front above, the central part of the event in the middle, and a late surge transporting a large boulder below (the one marked in Fig. 9)

Peak discharge and debris-flow volume have been computed separately for the three surges of the August 2011 event; the results are reported in Table 2. The total volume of the August 2011 event turns out to be about 2,400 m^3 (neglecting the inter-surge periods, likely transporting relatively little sediment, whose velocity assessment would hardly be possible). The sediment accumulated in the retention basin was determined by two topographic surveys carried out with a RIEGL LMS-Z620 terrestrial laser scanner (TLS) before (June 21, 2011) and after (September 15, 2011) the August 2011 debris flow. Point clouds were acquired with a spacing of 10 cm for the maximum scan radius (100 m) and an accuracy of 10 mm. To cover the entire area, each survey required three scan stations with a variable scan radius (from 50 to 100 m). The resulting point density allowed to derive two digital terrain models (DTMs) with a resolution of 0.5 m. As no other significant debris flows or floods with bedload have occurred in the Gadria and Strimm catchments in the period between the two TLS surveys, sediment deposition in the debris basin can be referred to the August 5 event. Figure 11 shows a map of the thickness of the deposits in the debris basin, computed as the difference between the DTMs resulting from the surveys of September and June 2011. Sediment volume accumulated in the debris basin resulted to be approximately 2,000 m^3. However, video recordings as well as post-event observations show that the trapping efficiency of the debris basin (ratio of sediment volume retained to the total incoming sediment) was well below 100 %. In fact, a remarkable amount of debris flowed through the slot opening of the retention check dam. The larger volume (about 400 m^3) estimated from the hydrographs, with respect to the deposited volume in the retention basin, is consistent with the outflow of part of the sediment through the check dam, as well as with sediment concentrations, being lower in the surges than in the deposits. In contrast, the sediment volumes discharged between the surges, and thus not calculated from the hydrographs, are reckoned to have a minor impact on the comparison.

As to the July 2013 event, this featured a much larger peak discharge than the August 2011 debris flow, as it was estimated between 80 and 90 m^3s^{-1} (depending whether the pre- or post-event D2 cross-section is used) compared to approximately 11 m^3s^{-1} (Table 2). The total debris-flow volume—based on Eq. 1 applied to eight surges identified within the hydrographs with the corresponding mean velocities—results to be about 10,000 m^3 at section D2 (using both pre- and post-event cross-sections). In contrast, the total volume when estimated using a mean flow velocity of the whole debris flow—computed by cross-correlation analysis—turns out considerably larger (about 15,000 m^3). If the front velocity was to be used, even higher volumes would be estimated, given its higher value (5.7 vs. 5.0 ms^{-1}). It is worth to point out that if the horizontal distance (75 m) between the two radar sensor was used instead of the actual inclined flow path (80 m) used in the all the calculations presented above, velocity, discharge and volumes estimation would overall decrease by 5–7 %.

The topographical assessment of the sediment volume trapped in the retention basin during the 2013 event was carried out applying the same TLS methodology described for the 2011 event, i.e., by subtracting pre- and post-event surveys, and the result is about 8,000 m^3. This value indicates—as it could be expected—that debris-flow volume estimations carried out from hydrographs are definitely more accurate when the entire flow is subdivided into different surges, each having a different velocity, rather than using a single velocity, either calculated by cross-correlation on the whole event or by considering the front surge only. In any case, for both 2011 and 2013 events, the most reliable debris-flow volumes estimated from the hydrographs are slightly larger (10–20 %) than those from the topographical survey of sediment deposited in the retention basin. This is consistent with the fact that part of the debris flow was indeed observed to pass through the filter check dam, as well as the consideration of different water content/sediment concentrations between the moving debris flow and the deposited mass subsequently surveyed by TLS.

4.3 Soil moisture dynamics

The monitoring activities of hillslope hydrology (sites S1 and S2) permitted to obtain some useful insights into the soil moisture and piezometric dynamics in the Gadria basin, but to a lesser extent to what we hoped when they were planned. In fact, during the 3 years (2011–2013), pore pressure transducers in the three channel heads (site S1) did not record significant variations over time, not even during the July 2013 debris flow when high

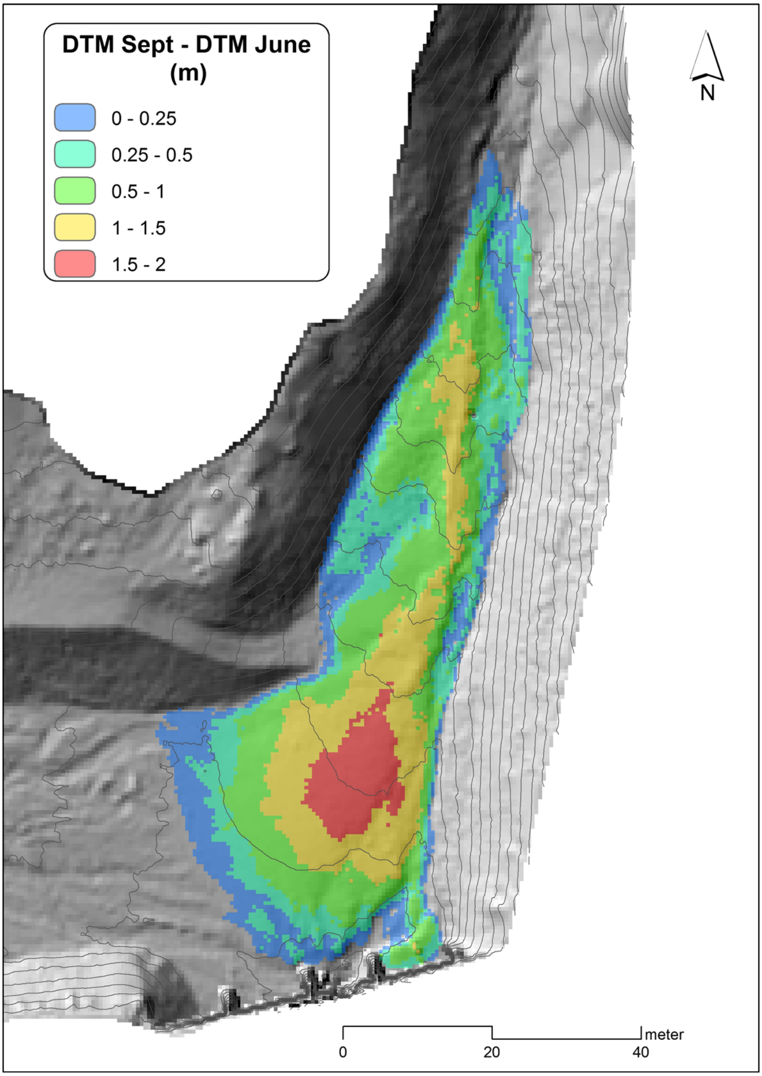

Fig. 11 Map of sediment thickness deposited in the retention basin after the August 2011 debris flow, evaluated as the difference between two TLS-derived DTMs. The contour interval is 1 m

rainfall intensities were measured at R1. This is likely a consequence of the high porosity characterizing the coarse substrate there (Fig. 5a, b) that leads to very high infiltration rates in this area. On the other hand, the installation of pore pressure transducers in such conditions is quite challenging, and their spatial representativeness and reliability through time are probably low. In October 2013, these pressure transducers were removed from the ground with the aim to re-install them in 2014 at nearby sites featuring bedrock at limited depths in the very proximity of the main channel.

Similarly, at site S2, the piezometers did not record any significant variation of groundwater level during the study period. This is likely due to the shallow depth at which they were installed (about 1 m), probably not sufficient to intercept the transient water table rise (if any) even during the most important precipitation events. On the other hand, at site S2, the soil moisture probes did measure interesting data. A clear dependence of soil moisture variations on precipitation was observed, along with its marked variability in time, space and depth, as often occurs even at the small hillslope scale (e.g., Penna et al. 2013). In this paper, the local-scale spatial variation (i.e., within S2 site) is not analyzed and Fig. 12 illustrates the relative soil moisture variations derived from averaging hourly values recorded by 16 probes at two different depths (8 probes at 10 cm and 8 probes at 50 cm).

Examples of time series of average soil moisture for 3-week periods in July–August for each year of investigation (2011–2013) are reported in Fig. 12. For 2011 and 2013, these periods include the occurrence of the debris flows described in the previous sections, whereas for 2012, when no event occurred, a wetting-up period at the end of the summer was chosen. First of all, it is evident that soil moisture is higher at 10 cm depth compared to 50 cm and that the responses tend to be synchronous at the two depths (less clearly visible in 2011). This is likely a consequence of the relevant organic fraction present in the first centimeters of the soil profile at site S2, similarly to what observed in other Alpine sites (e.g., Penna et al. 2009), that also facilitates the rapid vertical percolation of rain water during precipitation events. Secondly, but very importantly, the 3 years exhibit marked differences in soil water content, with definitely wetter conditions and lower temporal variability during the few days antecedent the July and August 2011 debris flow compared to those preceding the July 2013 event, especially at 50 cm depth. The low rainfall amount and intensity associated with the August 2011 debris flow (see also Fig. 7) are visible, in particular relative to other storm events of the same year, but soil moisture during that event reached the maximum value recorded at 10 cm depth for the entire investigated periods. On the other hand, the smaller debris flow in July 2011 occurred at soil moisture conditions measured at 10 cm depth drier than those of the August 2011 event, whereas conditions at 50 cm were similar as they did not vary substantially over that period. As discussed in Sect. 4.1, precipitation for the August 2011 event is very likely underestimated, but high soil moisture conditions prior to the 5 August storm possibly favored debris-flow triggering even at a relatively low rainfall rate. In contrast, a remarkable storm during late August 2012 was not able to trigger any debris flow. This might be due to its insufficient rainfall intensity coupled to low antecedent soil moisture levels (Fig. 12). Notably, the July 18, 2013, debris flow occurred when soil moisture was low, especially at 50 cm depth, after a steady decline started in early July (Fig. 12). In this case, it is more likely that the very high intensity of the storm (Fig. 7) overrode the initially dry conditions being able to trigger the massive debris flow described in Sect. 4.2.

In Table 3 a summary of the main characteristics of the debris flows observed in the Gadria basin during the 2011–2013 period is reported.

5 Future perspectives

We would like to briefly outline the envisaged outcomes as well as the problems of this new instrumented site. The monitoring system installed in the Gadria catchment covers a channel reach immediately upstream of a retention basin—upstream of a filter check dam—as well as the retention basin itself. Filter check dams coupled to retention basins represent the most widespread structural measures for debris-flow control, thus their monitoring in terms of flow processes and deposition dynamics may provide evident

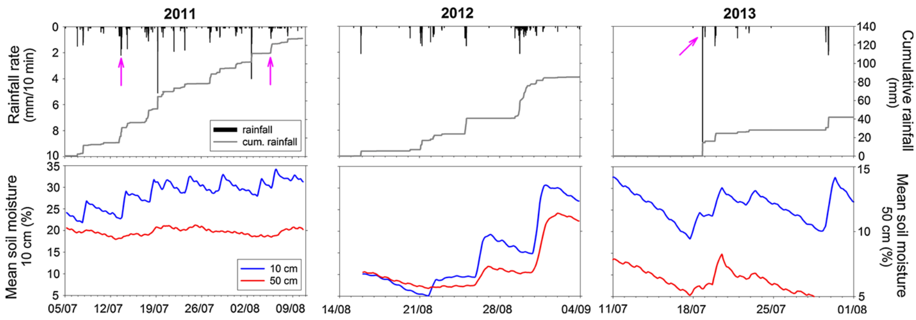

Fig. 12 Precipitation (measured at R1) and mean volumetric soil moisture at two soil depths (recorded at S2) during selected periods in the 3 years of investigation. The daily fluctuations visible in the soil moisture values are due to temperature effects. *Arrows* indicate the storms which triggered the debris flows occurred in the basin (July 13, 2011, August 5, 2011, July 18, 2013)

Table 3 Summary of the main characteristics of the debris flows occurred in the Gadria basin in the period 2011–2013

Date	Volume (m^3)	Max surge velocity ($m\ s^{-1}$)	Peak discharge ($m^3\ s^{-1}$)	Rainfall depth (mm)	Max rainfall intensity ($mm\ 10\ min^{-1}$)	Antecedent soil moisture conditions	Dominant channel changes
July 13, 2011	1,000*	–	–	5**	2.2	Intermediate	Deposition
August 5, 2011	2,400	2.6	11	9.4	0.9	Wet	Mixed
July 18, 2013	10,000	5.7	80–90	17.2	14.7	Intermediate	Erosion

The July 2011 event did not reach the monitoring station. A qualitative assessment of soil moisture conditions antecedent to each debris flow is provided based on soil moisture measurements at the S2 site relative to the range measured over the three summers (see Fig. 12)

* Based on channel deposition observed in the channel upstream of the station

** For the entire storm, whereas for the others it refers to the cumulative rainfall at the arrival of the debris-flow front

outcomes for improving the design and the operation of these structures (D'Agostino 2010). An interesting aspect of the debris-flow monitoring in the Gadria lies in the presence of the adjacent catchment, the Strimm basin. This features similar geological and lithological settings but quite different topographic characteristics, which lead to different types and intensity of sediment transport processes. The contemporary monitoring of debris flows in the Gadria and bedload transport floods in the Strimm [by means of morphological methods and clasts tagged with passive integrated transponders (PITs)] will provide new data and elements for understanding the variability of sediment transport processes in headwater channels of the Alps.

A possible problem that could affect the effective collection of experimental data is the frequency of debris flows in the Gadria catchment, which is high in the morphoclimatic context of the Italian Alps, but decidedly lower than in the most active debris-flow monitoring sites worldwide (e.g., Hu et al. 2011; Suwa et al. 2011). This implies the need for planning the monitoring in a long-term perspective to ensure collection of a database that would also permit recognition of possible variations in debris-flow response, possibly related to variations in debris availability or changes in climate forcing, and allow comparisons with other instrumented catchments. Finally, we have pointed out in the introduction the recent interest for debris-flow monitoring in Europe, which has led to the instrumentation of several catchments in the Alps and in the Pyrenees. The Gadria catchment aims at becoming part of a network of instrumented sites for debris-flow studies, in which the exchange and comparison of information on monitoring equipment, data processing methods and results will advance our understanding and capability to predict such natural hazards.

Acknowledgments The monitoring work has been conducted through the participation of the Department of Civil Protection of the Autonomous Province of Bozen-Bolzano to the EU Interreg IV B South East Europe—Project Monitor II (2010–2012) and thanks to the funding by the research project "GESTO" granted by the Autonomous Province of Bozen-Bolzano. Since September 2012, the monitoring activities are partly funded by the European Territorial Cooperation Alpine Space Programme 2007–2013 "SEDALP" and since March 2013 also by the research project "KINOFLOW" (granted by the Autonomous Province of Bozen-Bolzano). Rudolf Pollinger, Head of the Department of Hydraulic Engineering, Autonomous Province of Bozen-Bolzano, is warmly thanked for supporting the installation of the monitoring station. Stefan Hellweger, from the same Department, helped with the installation and management of the server and of the video cameras. Giancarlo Dalla Fontana, Director of the "CIRGEO" center (Padova), and Simone Calligaro are thanked for the availability and deployment of the TLS, respectively. We thank Austro Control (Austria) and Francesco Marra (University of Padova) for making available the radar rainfall estimates based on weather radar observations from the antenna in Valluga. We thank Enrico Buzzi, Raffaele Foffa, Alberto Gobbi, Nicola Mantese and Omar Oliviero for their support in soil hydrology monitoring. Ylenia Gelmini, Francesco Bettella, Enrico Pozza and Emilio Perina are finally thanked for their help in field surveys.

References

Arattano M (2003) Monitoring the presence of the debris flow front and its velocity through ground vibration detectors. In: Rickenmann D, Chen CL (eds) 3rd international conference on debris-flow hazard mitigation: mechanics, prediction and assessment. Millpress, Rotterdam, pp 719–730

Arattano M, Franzi L (2004) Analysis of different water-sediment flow processes in a mountain torrent. Nat Hazards Earth Syst Sci 4:783–791

Arattano M, Marchi L (2005) Measurements of debris flow velocity through cross-correlation of instrumentation data. Nat Hazards Earth Syst Sci 5(1):137–142

Arattano M, Marchi L (2008) Systems and sensors for debris-flow monitoring and warning. Sensors 8(4):2436–2452

Arattano M, Franzi L, Marchi L (2006) Influence of rheology on debris flow simulation. Nat Hazards Earth Syst Sci 6:519–528

Arattano M, Marchi L, Cavalli M (2012) Analysis of debris-flow recordings in an instrumented basin: confirmations and new findings. Nat Hazards Earth Syst Sci 12(3):679–686

Bacchini M, Zannoni A (2003) Relations between rainfall and triggering of debris-flow: case study of Cancia (Dolomites, Northeastern Italy). Nat Hazards Earth Syst Sci 3(1–2):71–79

Badoux A, Graf C, Rhyner J, Kuntner R, McArdell BW (2009) A debris-flow alarm system for the Alpine Illgraben catchment: design and performance. Nat Hazards 49(3):517–539

Bargossi GM, Bove G, Cucato M, Gregnanin A, Morelli C, Moretti A, Poli S, Zanchetta S, Zanchi A (2010) Note illustrative della Carta Geologica d'Italia. Foglio 013—Merano. ISPRA, Servizio Geologico d'Italia

Berger C, McArdell BW, Schlunegger F (2011) Direct measurement of channel erosion by debris flows, Illgraben, Switzerland. J Geophys Res Earth Surf 116:F01002. doi:10.1029/2010JF001722

Brardinoni F, Church M, Simoni A, Macconi P (2012) Lithologic and glacially conditioned controls on regional debris-flow sediment dynamics. Geology 40(5):455–458

Caine N (1980) The rainfall intensity-duration control of shallow landslides and debris flows. Geogr Ann A 62:23–27

Cavalli M, Trevisani S, Comiti F, Marchi L (2013) Geomorphometric assessment of spatial sediment connectivity in small Alpine catchments. Geomorphology 188:31–41
Chang SY (2003) Evaluation of a system for detecting debris flows and warning road traffic at bridges susceptible to debris-flow hazard. In: Rickenmann D, Chen C (eds) 3rd international conference on Debris-flow hazards mitigation: mechanics, prediction, and assessment. Millpress, Rotterdam, pp 731–742
Coe JA, Kinner DA, Godt JW (2008) Initiation conditions for debris flows generated by runoff at Chalk Cliffs, central Colorado. Geomorphology 96(3–4):270–297
D'Agostino V (2010) Filtering-retention check dam design in mountain torrents. In: Conesa CC, Lenzi MA (eds) Check dams, morphological adjustments and erosion control in torrential streams. Nova Science, New York, pp 185–210
Fischer K (1965) Murkegel, Schwemmkegel und Kegelimse in den Alpentalern. Mitteilungen der Geographischer Gesellschaft in Munchen 56:127–159
Frei C, Schär C (1998) A precipitation climatology of the Alps from high-resolution rain-gauge observations. Int J Climatol 18(8):873–900
Guzzetti F, Stark CP, Salvati P (2005) Evaluation of flood and landslide risk to the population of Italy. Environ Manag 36(1):15–36
Guzzetti F, Peruccacci S, Rossi M, Stark CP (2008) The rainfall intensity-duration control of shallow landslides and debris flows: an update. Landslides 5(1):3–17
Habler G, Thöni M, Grasemann B (2009) Cretaceous metamorphism in the Austroalpine Matsch Unit (Eastern Alps): the interrelation between deformation and chemical equilibration processes. Mineral Petrol 97(3–4):149–171
Hilker N, Badoux A, Hegg C (2009) The Swiss flood and landslide damage database 1972–2007. Nat Hazards Earth Syst Sci 9(3):913–925
Hu K, Hu C, Li Y, Cui P (2011) Characteristics and mechanism of debris-flow surges at Jiangjia Ravine. In: Genevois R, Hamilton DL, Prestininzi A (eds) 5th international conference on debris-flow hazards mitigation: mechanics, prediction and assessment. Casa Editrice Università La Sapienza, Roma, pp 211–217
Huang C, Yin H, Chen C, Yeh CH, Wang CL (2007) Ground vibrations produced by rock motions and debris flows. J Geophys Res 112:F02014
Hungr O, Morgan GC, Van Dine DF, Lister RD (1987) Debris flow defenses in British Columbia. In: Costa JE, Wieczorek GF (eds) Debris flows/avalanches: process, recognition, and mitigation. Geological Society of America, Reviews in Engineering Geology 7:201–222
Hungr O, Evans SG, Bovis MJ, Hutchinson JN (2001) A review of the classification of landslides in the flow type. Environ Eng Geosci 7(3):221–228
Hungr O, McDougall S, Bovis M (2005) Entrainment of material by debris flows. In: Jakob M, Hungr O (eds) Debris-flow hazards and related phenomena. Springer, Berlin, pp 135–158
Hürlimann M, Rickenmann D, Graf C (2003) Field and monitoring data of debris-flow events in the Swiss Alps. Can Geotech J 40(1):161–175
Hürlimann M, Abancó C, Moya J, Raïmat C, Luis-Fonseca R (2011) Debris-flow monitoring stations in the Eastern Pyrenees. Description of instrumentation, first experiences and preliminary results. In: Genevois R, Hamilton DL, Prestininzi A (eds) 5th international conference on debris-flow hazards mitigation: mechanics, prediction and assessment. Casa Editrice Università La Sapienza, Roma, pp 553–562
Jarman D, Agliardi F, Crosta GB (2011) Megafans and outsize fans from catastrophic slope failures in Alpine glacial troughs: the Malser Haide and the Val Venosta cluster, Italy. Geol Soc Lond Spec Publ 351:253–277
Kogelnig A, Hübl J, Suriñach E, Vilajosana I, McArdell B (2014) Infrasound produced by debris flow: propagation and frequency content evolution. Nat Hazards 70(3):1713–1733. doi:10.1007/s11069-011-9741-8
LaHusen R (1996) Detecting debris flows using ground vibrations. USGS Fact Sheet 236-96, USGS (ed)
Lollino G, Arattano M, Cuccureddu M (2002) The use of the automatic inclinometric system for landslide early warning: the case of Cabella Ligure (North-Western Italy). Phys Chem Earth 27(36):1545–1550. doi:10.1016/S1474-7065(02)00175-4
Lollino G, Arattano M, Allasia P, Giordan D (2006) Time response of a landslide to meteorological events. Nat Hazards Earth Syst Sci 6(2):179–184
Mao L, Cavalli M, Comiti F, Marchi L, Lenzi MA, Arattano M (2009) Sediment transfer processes in two Alpine catchments of contrasting morphological settings. J Hydrol 364(1–2):88–98
Marchi L, Arattano M, Deganutti AM (2002) Ten years of debris-flow monitoring in the Moscardo Torrent (Italian Alps). Geomorphology 46(1–2):1–17

McArdell BW, Badoux A (2007) Influence of rainfall on the initiation of debris flows at the Illgraben catchment, canton of Valais, Switzerland. Geophys Res Abstr 9:08804

McArdell BW, Bartelt P, Kowalski J (2007) Field observations of basal forces and fluid pore pressure in a debris flow. Geophys Res Lett 34(7):L07406

McCoy SW, Kean JW, Coe JA, Staley DM, Wasklewicz TA, Tucker GE (2010) Evolution of a natural debris flow: in situ measurements of flow dynamics, video imagery, and terrestrial laser scanning. Geology 38:735–738. doi:10.1130/G30928.1

Navratil O, Liébault F, Bellot H, Theule J, Travaglini E, Ravanat X, Ousset F, Laigle D, Segel V, Fiquet M (2012) High-frequency monitoring of debris flows in the French Alps. In: Proceedings of 12th interpraevent congress, Grenoble, 281–291

Navratil O, Liébault F, Bellot H, Travaglini E, Theule J, Chambon G, Laigle D (2013) High-frequency monitoring of debris-flow propagation along the Réal Torrent, Southern French Prealps. Geomorphology 201:157–171

Okuda S, Suwa H, Okunishi K, Yokoyama K, Nakano M (1980) Observations on the motion of a debris flow and its geomorphological effects. Z für Geomorphol Suppl 35:142–163

Parajka J, Kohnova S, Balint G, Barbuc M, Borga M, Claps P, Cheval S, Dumitrescu A, Gaume E, Hlavcova K, Merz R, Pfaundler M, Stancalie G, Szolgay J, Bloschl G (2010) Seasonal characteristics of flood regimes across the Alpine–Carpathian range. J Hydrol 394(1–2):78–89

Penna D, Borga M, Norbiato D, Dalla Fontana G (2009) Hillslope scale soil moisture variability in a steep alpine terrain. J Hydrol 364:311–327

Penna D, Brocca L, Borga M, Dalla Fontana G (2013) Soil moisture temporal stability at different depths on two alpine hillslopes during wet and dry periods. J Hydrol 477:55–71

Pierson TC (1986) Flow behavior of channelized debris flows, Mount St. Helens, Washington. In: Abrahms AD (ed) Hillslope processes. Allen & Unwin, Boston, pp 269–296

Ratschbacher L (1986) Kinematics of Austro-Alpine cover nappes: changing translation path due to transpression. Tectonophysics 125:335–356

Rickenmann D, Turowski JM, Fritschi B, Klaiber A, Ludwig A (2012) Bedload transport measurements at the Erlenbach stream with geophones and automated basket samplers. Earth Surf Proc Land 37(9):1000–1011

Solva H, Grasemann B, Thöni M, Thiede R, Habler G (2005) The Schneeberg normal fault zone: normal faulting associated with Cretaceous SE-directed extrusion in the Eastern Alps (Italy/Austria). Tectonophysics 401(3–4):143–166

Staley DM, Kean JW, Cannon SH, Schmidt KM, Laber JL (2013) Objective definition of rainfall intensity-duration thresholds for the initiation of post-fire debris flows in southern California. Landslides 10:547–563. doi:10.1007/10346-012-0341-9

Suwa H, Okano K, Kanno T (2011) Forty years of debris flow monitoring at Kamikamihorizawa Creek, Mount Yakedake, Japan. In: Genevois R, Hamilton DL, Prestininzi A (eds) 5th international conference on debris-flow hazards mitigation: mechanics, prediction and assessment. Casa Editrice Università La Sapienza, Roma, pp 605–613

Tecca PR, Galgaro A, Genevois R, Deganutti AM (2003) Development of a remotely controlled debris flow monitoring system in the Dolomites (Acquabona, Italy). Hydrol Process 17(9):1771–1784

Theule JI, Liébault F, Loye A, Laigle D, Jaboyedoff M (2012) Sediment budget monitoring of debris-flow and bedload transport in the Manival Torrent, SE France. Nat Hazards Earth Syst Sci 12:731–749

Thöni M (1999) A review of geochronological data from the Eastern Alps. Schweiz Mineral Petrogr Mitt 79(1):209–230

Wilson RC, Mark RK, Barbato G (1993) Operation of a real-time warning system for debris flows in the S. Francisco Bay Area, California. In: Hsieh Wen Shen, S. T. Su e Feng Wen (eds), Hydraulic engineering '93 vol 2, ASCE 1993 national conference on hydraulic engineering and international symposium on engineering hydrology. American Society of Civil Engineers, New York, pp 1592–1597

Yin HY, Huang CJ, Chen CY, Fang YM, Lee BJ, Chou TY (2011) The present development of debris flow monitoring technology in Taiwan—a case study presentation. In: Genevois R, Hamilton DL, Prestininzi A (eds) 5th international conference on debris-flow hazards mitigation: mechanics, prediction and assessment. Casa Editrice Università La Sapienza, Roma, pp 623–631

Zhang S (1993) A comprehensive approach to the observation and prevention of debris flows in China. Nat Hazards 7(1):1–23